

# Small Object Detection Model with Spatial Laplacian Pyramid Attention and Multi-Scale Features Enhancement in Aerial Images

Zhangjian Ji, Huijia Yan, Shaotong Qiao, Kai Feng and Wei Wei *Member, IEEE*,

**Abstract**—Detecting objects in aerial images confronts some significant challenges, including small size, dense and non-uniform distribution of objects over high-resolution images, which makes detection inefficient. Thus, in this paper, we proposed a small object detection algorithm based on a Spatial Laplacian Pyramid Attention and Multi-Scale Feature Enhancement in aerial images. Firstly, in order to improve the feature representation of ResNet-50 on small objects, we presented a novel Spatial Laplacian Pyramid Attention (SLPA) module, which is integrated after each stage of ResNet-50 to identify and emphasize important local regions. Secondly, to enhance the model’s semantic understanding and features representation, we designed a Multi-Scale Feature Enhancement Module (MSFEM), which is incorporated into the lateral connections of C5 layer for building Feature Pyramid Network (FPN). Finally, the features representation quality of traditional feature pyramid network will be affected because the features are not aligned when the upper and lower layers are fused. In order to handle it, we utilized deformable convolutions to align the features in the fusion processing of the upper and lower levels of the Feature Pyramid Network, which can help enhance the model’s ability to detect and recognize small objects. The extensive experimental results on two benchmark datasets: VisDrone and DOTA demonstrate that our improved model performs better for small object detection in aerial images compared to the original algorithm.

**Index Terms**—Small object detection, Laplacian pyramid spatial attention, Multi-scale features enhancement, Dilatational convolution, Deformable convolution.

## I. INTRODUCTION

**O**BJECT detection is a fundamental task in modern computer vision, aiming to accurately identify and locate specific objects in images or videos. This task plays a crucial role in a wide range of applications, including but not limited to autonomous driving, video surveillance, disaster search and medical imaging analysis. In recently years, with the development of deep learning technology, some typical object detection methods (e.g., FasterRCNN [1], YOLO [2], SSD[3], CornerNet[4] and RetinaNet) have obtained significant success in nature images (e.g., MS COCO and Pascal VOC). However, these methods can not obtain satisfactory results in aerial images. The main reasons include three aspects: (1) the aerial images usually compose of lots of small scale objects; (2) targets are sparsely and non-uniformly distributed in the whole

aerial image; (3) the number of targets of different categories is grossly unbalanced in aerial images.

Compared with targets in nature images, these challenges mentioned above cause that the existing most object detection methods based on the deep network can not extract effective feature representation for small objects in aerial images because of the features down-sampling in ConvNets. In order to handle it, early works [5], [6] mainly increase the resolution of feature map by inputting the high-resolution images or reducing the down-sampling rate of network model so as to improve the detection performance of small objects in aerial images. However, simply expanding the resolution of feature maps will impose a huge computational burden, and can not meet the needs of practical applications.

To utilize the higher resolution and reduce the information loss, a popular direction is to crop the original image into small patches, then resize these patches to the size of input image required by the network model and perform object detection on them, such as uniform cropping [7], density cropping [8], [9] and Cascaded Zoom-in (CZ) detector [10]. The uniform cropping can help improve the detection accuracy of small objects, but the results achieved by it are not optimal because it does not consider the distribution of the objects for cropping, leading to a majority of cropping patches only contain the background or large objects may be cut into two or more different cropping patches. As the objects in aerial images are usually sparsely and non-uniform distributed, an intuitive way to crop the patches is to utilize the additional learnable modules (such as density maps [9] and cluster proposal networks [8]) to perform density-based cropping. This usually needs additional components in the network model, often with multiple stages of training. Thus, although the performance of density crop-based methods is better, practitioners still widely employ uniform cropping because of practical simplicity it offers. In order to bridge the gap between research and practice, the CZ detector [10] can utilize density crops within the training of a standard detector, offering the simplicity of uniform cropping, yet providing the benefits of density crops. Therefore, in this paper, we select the CZ detector as our basic framework.

In addition, existing studies have shown that the quality of features representation is very crucial to the performance of object detection, and current most object detection methods based on the deep learning are not able to extract the effective features for small objects. Therefore, another feasible direction is to enhance the features representations of small objects

Zhangjian Ji, Huijia Yan, Shaotong Qiao, Kai Feng and Wei Wei are with the Key Laboratory of Computational Intelligence and Chinese Information Processing of Ministry of Education, School of Computer and Information Technology, Shanxi University, Taiyuan 030006, China E-mail: {jizhangjian@sxu.edu.cn}

by improving the backbone and neck networks of object detection model. For the backbone network, some researchers introduce the channel attention module [11], spatial attention module [12] or convolutional block attention module [13] to enhance its features representation power. Nonetheless, with the increase of the layer number in the backbone, the downsampling operations make the resolution of features map reduce, which weakens the features representation of small objects. Thus, in order to address this issue, inspired by the image super-resolution network architecture in [14], we proposed a lightweight spatial laplacian pyramid attention module, which can be plugged into each stage of the backbone network (e.g. ResNet50) to heighten the representation power of small objects. For most object detection models, the Feature Pyramid Network (FPN) is a common network structure used in neck networks and it can generate the different scales feature maps with rich semantic information to detect objects of varying sizes. However, FPN may underperform when detecting small objects. This limitation arises from the loss of fine details of small objects during the top-down multi-scale feature fusion, often caused by downsampling operations such as pooling or large-stride convolutions. As a result, small objects are represented with less precision on feature maps, often appearing blurred and undersized. Additionally, lower-level feature maps in FPN may not provide sufficient resolution to accurately detect small objects, while higher-level feature maps may lack rich semantic information, making it difficult for the model to differentiate between small objects of different categories. To handle this problem, we designed a multi-scale feature enhancement module to augment the features on the C5 layer, under the guidance of adaptive convolution with different dilation rates. Thereby, when the feature maps in FPN are fused from the top-down method, it can effectively enhance the feature representation of small objects. For the sake of clarity, the main contributions of this work can be summarized as follows:

- After each stage of ResNet-50, we integrate a novel Spatial Laplacian Pyramid Attention (SLPA) module to create an enhanced backbone, which can highlight crucial local regions in the image to boost its features representation power.
- To avoid the information loss from the top-down fusion in FPN, a Multi-Scale Feature Enhancement Module (MSFEM) is incorporated into the lateral connection of C5 layer to build the new feature pyramid network, which can help the model capture the critical detail information in the image so as to enhance its semantic understanding and features representation power.
- For the fusing processing of Feature Pyramid network, we utilize the deformation convolutions to align the features of its upper and lower layers, which enables to enhance the model's ability to detect and recognize small objects.
- Quantitative experiments and ablation study on two benchmark datasets demonstrate that our improved model performs better for small object detection in aerial images compared to the original algorithm.

The remainder of this paper is organized as follows: Section

II reviews the related works, in Section III, we introduce the proposed methodology in details, Section IV presents and analyzes the findings from the ablation studies as well as the comparison experiments, and the conclusions in this work are given in Section V.

## II. RELATED WORKS

### A. Object Detection

With the rise of deep learning, object detection methods based on deep learning have been dominated in the field of natural image object detection. According to the pipeline of object detection methods, they can be roughly categorized into two streams: two-stage [1], [15], [16] and one-stage [2], [3], [17], [18] object detectors. Two-stage detectors separate object detection into two steps including region generation and region-wise classifier. Earlier two-stage methods (e.g., RCNN [16]) first generate the candidate regions of the targets, and then extract the features of these RoIs and classify them, which are not end-to-end trainable models. Subsequently, a learnable component known as the Region Proposal Network (RPN) is presented for extracting the candidate regions, giving birth to end-to-end trainable two-stage object detectors [1], [15]. In contrast, one-stage object detection methods [2], [18] don't need to extract the RoIs and classify and regress directly from the anchor boxes. They are easy deployment and applicable to real-time object detection. But generally speaking, due to utilize the RoAlign operation to align the object's features explicitly, two-stage methods tend to be more accurate than one-stages ones and hence used more in aerial detection [19], [9], [20], [21]. Recently, as deep learning techniques continue to evolve, one-stage detectors have narrowed the performance gap with two-stage ones. Thus, they are being exolored in aerial images [22], [23]. Nowadays, anchor-free detectors [24], [17], [25], [4] have become very popular, since they avoid to hand-craft anchor box dimensions and spend extra time matching them. Thus, in [22], the authors also attempt to apply their detection framework on anchor-free FCOS [17]. In this paper, for a fair comparison with existing methods, we mainly perform our study on the two-stage detectors.

### B. Small Object Detection in aerial images

In addition to natural images, object detection has been widely applied in aerial images. However, most of existing ordinary object detection methods can not achieve the desired detection performance because aerial images contain lots of small scale objects that are sparsely and non-uniformly distributed. In order to handle the inadequacy of information problem for small object detection, many researchers have undertaken extensive work in this field. According to different technical routes, these works can be categorized into: scale-aware training [26], [27], [22], [28], [29], super-resolution methods [5], [6], [30], context-modeling [31], [32], [33], [34], focus-and-detection [10], [8], [9], [20], [19], [35], [36], [37] and so on. Due to the sparse and non-uniform distribution of small objects in the high-resolution aerial images, for small object detection in aerial image, density cropping is a popular method, such as ClusDet [8], DMNet [9], CDMNet [20] and

so on. These methods can guarantee that small objects are processed at higher resolutions, thereby reducing the information loss and improving the performance of subsequent object detection. However, they generally need to training the additional focus-detecting model to generate the candidate regions, which are more complex to use than uniform cropping. Different from those, The CZDet [10] re-purposes the detector itself to extract the density cropping regions, thereby eliminating the need for an additional learnable module.

### C. Attention Mechanisms

Attention mechanisms that mimic the human visual system play a critical role in deep neural networks, helping the network focus on the regions of interest that are beneficial for decision-making in images. This mechanism has been successfully applied in various tasks, such as object detection [38] and semantic segmentation [39]. For instance, the early attention models, e.g. SENet [11], it introduces channel-wise attention module that calculated via global average-pool operation to exploit the inter-channel relationship. However, it only obtains the suboptimal features because of missing the spatial attention that plays an important role in deciding 'where' to focus. The CBAM [13], which is a representative model of mixture attention mechanisms, composes of spatial and channel-wise attention modules and is superior to the SENet [11] that only using the channel-wise attention. But these two models lack the pow of global context modeling effectively enough, the GCNet, combing the optimal implementation of each step of simplified non-local block [40] and SE block [11], can effectively model the global context, with the lightweight property of SENet [11]. Thus, like SE block, GCNet can be also applied in all residual blocks of the ResNet architecture. Although these attention modules mentioned above achieve certain performance gains on many visual tasks, they are not specifically designed for object detection. To improve the performance of object detection, Li *et al.* [38] propose a MAD unit to aggressively search for neuron activations among feature maps from both low-level and high-level streams. In addition, most of existing object detection methods only rely on recognizing object instances individually, without exploiting their relations during learning. In fact, besides the contextual information, the relation between objects can also help object detection and recognition, so Hu *et al.* [41] propose an adapted attention module to model the relations between objects for object detection. Unfortunately, for small object detection in aerial images, these attention models mentioned above do not perform well because downsampling operations make small objects miss lots of useful information. Thus, in order to handle this issue, inspired by the image super-resolution network architecture in [14], we design a lightweight spatial laplacian pyramid attention module, which can be embedded into each stage of the backbone (e.g. ResNet50) to enhance the features representation power of small objects.

### D. Multi-Scale Feature Enhancement

Multi-scale feature enhancement addresses the issue of varying object scales by acquiring and fusing features at

multiple scales, thereby improving the final detection results. For example, in order to boost the performance of object detection, Lin *et al.* [26] first proposed a feature pyramid network (FPN) for feature representation, which combines the low-level location features in shallow layers with high-level semantic features in deep layers. Subsequently, in order to further improve the feature presentation power of FPN, many researchers make every effort to ameliorate the structure of FPN by adding the additional pathways to further fuse deep and shallow features or incorporating attention mechanisms to guide the fusion of features across different layers. E.g., AC-FPN [42] utilizes dilated convolutions of different rates to capture semantic information from the highest feature layers by fully integrating attention guidance, and PANet [43] adds an additional bottom-up pathway on top of FPN, which achieves better performance than FPN, but with the cost of more parameters and computations. To improve the efficiency of the model, Bi-FPN [44] introduces weighted bi-directional cross-scale connections based on PANet to balance information across different scales. TridentNet [27] leverages dilated convolutions to build parallel multi-branch structures with different receptive fields, handling object scale variation in detection tasks through scale-aware training. AugFPN [45] adopts a consistency supervision approach to narrow the semantic gaps between different scale features before multi-scale features fusion, reducing information loss in the highest level of FPN. Although those methods mentioned above boost the accuracy of object detection in natural images, their limitations arise when it is expected to capture the densely tiny object in aerial images. Thus, in this paper, under the guidance of adaptive convolution with different dilation rates, we design a multi-scale feature enhancement module to build a new feature pyramid network, which can help the model capture the critical detail information of images to facilitate small objects detecting.

## III. PROPOSED METHOD

In this section, we mainly describe our two basic modules that designed specifically to improve the detection performance for small objects in detail and how it can be plugged into existing small object detection methods.

### A. Improved Object Detection Framework

The FasterRCNN-FPN, as a two-stage object detector, has been widely used in lots of aerial image object detection models, e.g., ClusDet [8], DMNet [9], CDMNet [20], CZDet [10] and so on. However, due to containing plenty of small or even tiny objects in aerial images, the backbone network (e.g., ResNet) and neck network (e.g., FPN) that adopted in FasterRCNN are not able to extract the effective features for them. Therefore, a feasible direction is to enhance its ability to detect small objects by modifying the architecture of backbone and neck networks in FasterRCNN. For the backbone network, inspired by the image super-resolution network architecture in [14], we designed a lightweight Spatial Laplacian Pyramid Attention (SLPA) module, which can be plugged into most backbone networks to boost their features representation power

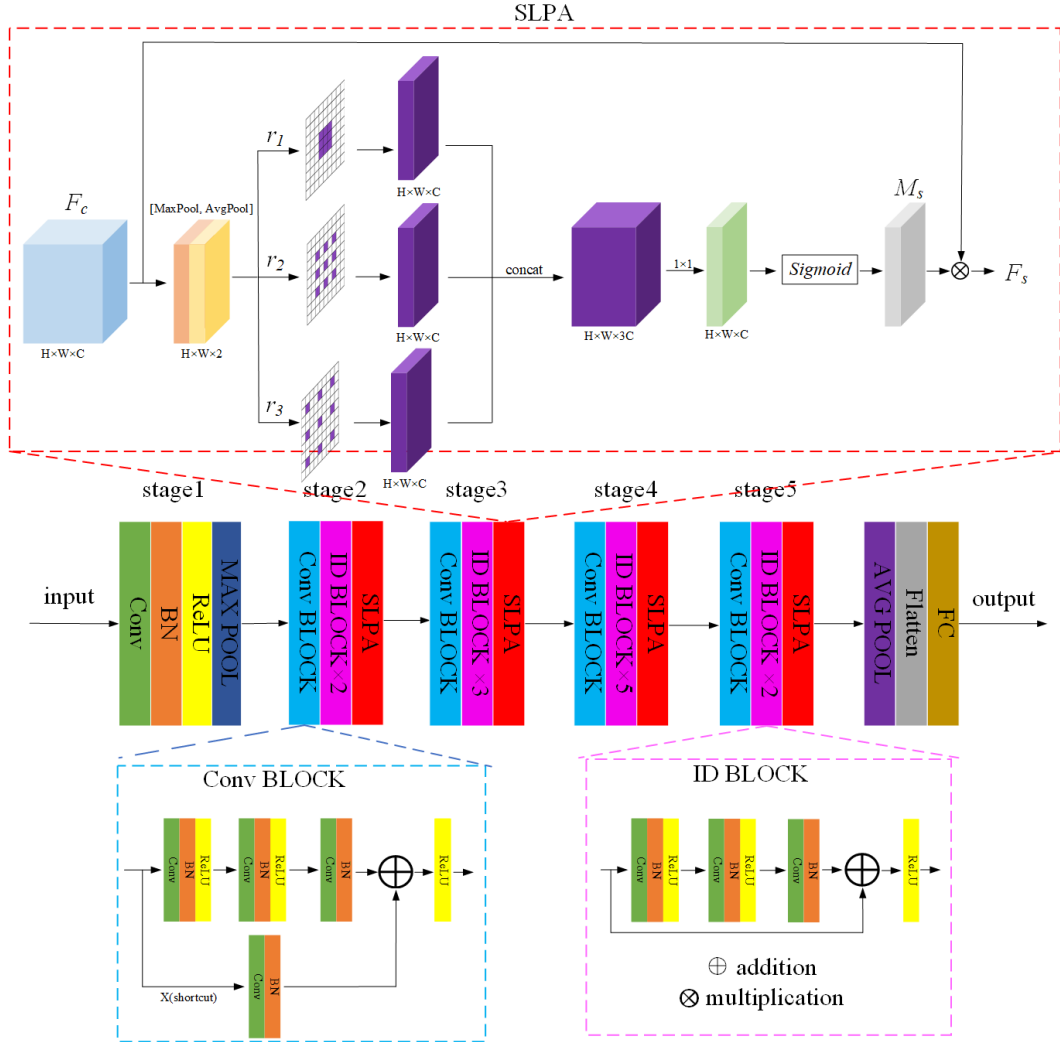


Fig. 1: The improved ResNet50 architecture after inserting our proposed SLPA module.

for small objects. Taking the ResNet50 as an example, our proposed SLPA module is embedded into its each stage, that is, the improved ResNet50 is shown in Figure 1. For the neck network, the FPN is a common network structure and it can generate the different scales features maps with rich semantic information to detect the objects of varying sizes. However, when perform the top-down feature fusion in FPN, the top-layer feature suffers from some information loss because its channel number decreases, which severely impairs its feature representation capability. Therefore, in order to enhance its feature representation power for small objects, we design a multi-scale feature enhancement module to insert the lateral connection of  $C_5$  layer of FPN, which extracts and fuses the diverse information of the top-layer feature. Sequently, we improve its architecture by replacing the FPN of FasterRCNN-FPN with our new FPN module, which is shown in Figure 2.

### B. Spatial Laplacian Pyramid Attention Module

With the increase of layer number in the backbone (e.g., ResNet), the ever-shrinking features map weakens the features

representation for small objects. In order to enhance the features representation of small objects and capture more subtle features, inspired by the image super-resolution network architecture in [14], we designed a lightweight Spatial Laplacian Pyramid Attention (SLPA) module, which is shown in Figure 1.

As is shown in the SLPA module of Figure 1, firstly, the input features  $F_c \in \mathbb{R}^{H \times W \times C}$  is compressed from C-dimensional channels to 2-dimensional channels via the Max-Pool and AvgPool, which can be repressed as

$$F' = \text{concat}(\text{MaxPool}(F_c), \text{AvgPool}(F_c)), \quad (1)$$

where  $\text{concat}(\cdot, \cdot)$  denotes the merging of two feature tensors.

Next, to capture the contextual information at the Laplacian Pyramids, we use the ReLU and the different dilation rates convolutional layers to learn the critical features at different scales as follow:

$$f_i = \text{ReLU}(r_i(F')), (i = 1, 2, 3), \quad (2)$$

where  $r_i$  denotes the dilation convolution and its dilation rate is specified by the subscripts. The multi-level features  $f_1, f_2, f_3$  obtained from  $F'$  are concatenated as  $Z = [f_1; f_2; f_3]$ .

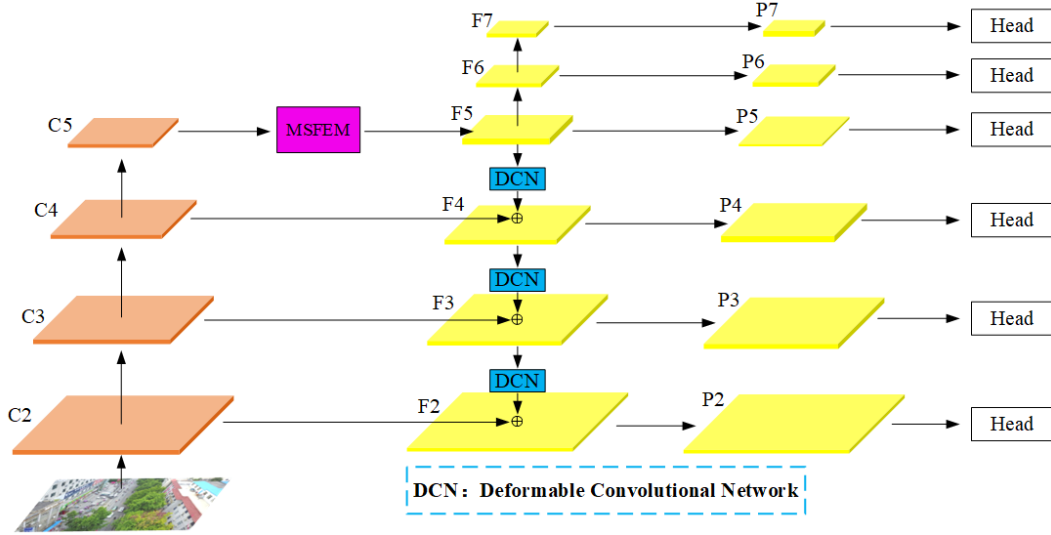


Fig. 2: The architecture of the improved FasterRCNN-FPN.

Furthermore, to produce the attention map,  $Z$  is fed into  $1 \times 1$  convolution operation  $Conv_{1 \times 1}$  followed by the sigmoid activation as:

$$M_s = \text{Sigmoid}(Conv_{1 \times 1}(Z)). \quad (3)$$

Finally, the input  $F_c$  of the Spatial Laplacian Pyramid Attention (SLPA) is adaptively rescaled by the attention map  $M_s$  as:

$$F_s = F_c \times M_s. \quad (4)$$

### C. Multi-scale Features Enhancement Module

Top-down feature fusion in FPN is performed by using the  $C_5$  layer feature. However, the  $C_5$  layer feature only contains the semantic information for the specific receptive field but is incompatible with other feature maps. Thus, inspired by adaptive convolution kernels [46], we consider using them to perform the multi-scale feature enhancement for the  $C_5$  layer feature. For this purpose, we design the module shown in the following Figure 3. Firstly, in our proposed module, in order to perform multi-scale feature enhancement, we split the  $Y$  feature channels output by the  $C_5$  layer into four groups and use adaptive convolution to convolve each group with different dilation rates [47]. Meanwhile, the global information of the  $C_5$  layer is also obtained by an adaptive global average pooling. Next, to ensure that the sufficient feature information is contained, we concatenate the original features  $Y$ , grouping feature after processed by adaptive convolution and the global information that obtained by an adaptive global average pooling. Finally, we perform a  $1 \times 1$  convolution to allow better integration of feature information. Thus, our proposed multi-scale feature enhance module can be formulated as follows:

$$y_i = \begin{cases} Y, & i = 0 \\ \sigma(\text{Adconv}_r(\text{split}(Y))), & i, r \in \{1, 2, 3, 4\} \\ U_s(\text{AAP2d}(Y)), & i = 5 \end{cases} \quad (5)$$

$$\text{output} = Conv_{1 \times 1}(\text{concat}([y_0, y_1, y_2, y_3, y_4, y_5])) \quad (6)$$

where  $\text{split}(\cdot)$  represents a grouping function, which divides the  $Y$  feature into four groups along the channel;  $\sigma(\cdot)$  denotes the Leaky ReLU activation function;  $\text{AAP2d}(\cdot)$  represents the adaptive average pooling operation;  $U_s$  denotes the upsampling operation;  $\text{Adconv}_r(\cdot)$  defines the adaptive dilation convolution with different dilation rates.

The adaptive dilation convolution module adopts the dual-branch structure to learn the contextual information around each pixel (seeing the adaptive convolution process of the Figure 3). In the upper branch, we compress the input feature  $X \in \mathbb{R}^{N \times C \times W \times H}$  to the size of adaptive convolution kernel ( $X1 \in \mathbb{R}^{N \times k * k \times W \times H}$ ,  $k$  denotes the kernel size), which obtains the surrounding contextual information on each pixel. After that, we go through a batch normalization layer and a softmax activation layer to obtain the features with surrounding contextual information and take out the feature pixel by pixel on  $k \times k$  channels to expand into  $k * k$  convolution kernel size. Finally, we reshape the dimensions of features to obtain the adaptive convolution kernel parameters  $X2 \in \mathbb{R}^{N \times g \times k * k \times H * W}$  ( $g$  denotes the number of groups of convolution kernel channels), which can be formulated as:

$$X2 = \text{reshape}(\text{Softmax}(\text{Bn}(Conv_{3 \times 3}(X1)))). \quad (7)$$

In Eq.7, the  $Conv_{3 \times 3}$  represents the convolution operation with a convolution size of 3. The  $\text{Bn}$  is batch normalization.

Next, in the lower branch, the input feature  $X \in \mathbb{R}^{N \times C \times W \times H}$  is expanded pixel by pixel to  $k * k$  size, obtaining  $X3 \in \mathbb{R}^{N \times C \times k * k \times W * H}$ . Finally, we adopt the adaptive convolution kernel parameters  $X2 \in \mathbb{R}^{N \times g \times k * k \times H * W}$  obtained by the Eq.7 to perform convolution on the same spatial location of  $X3$ , *i.e.*

$$Y_{i,j} = \text{reshape}(\sum_{p \in \Omega} X2_{p,i * W + j} \cdot X3_{p,i * W + j}), \quad (8)$$

where  $Y_{i,j}$  denotes the output features of convolution at pixel location  $(i, j)$ , and  $p \in \Omega := \{1, 2, \dots, k * k\}$  denotes the pixel index within the range of convolution.

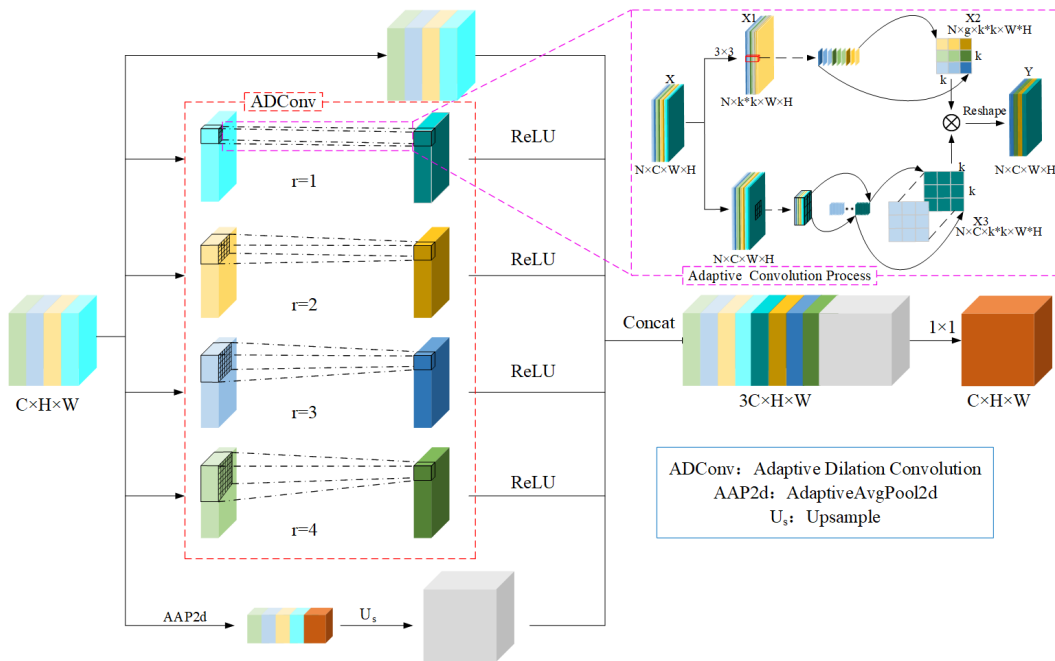


Fig. 3: The whole process of multi-scale feature enhancement module.

#### IV. EXPERIMENTS

In this section, we first introduce the benchmark datasets and evaluation metrics used in our experiments. Next, we describe the implementation details. Then, we compare the proposed SLPA module and the existing CBAM, and conduct ablation study to analyze the effectiveness of the proposed two modules (SLPA and MSFEM) and the effect of different dilation rates in them. Finally, we compare the improved CZ Det that integrates the proposed SLPA and MSFEM with the original CZ Det and other existing state-of-the-art and the most related object detection methods on VisDrone and DOTA-v1.0 datasets.

##### A. Experimental setup

**Datasets.** To assess the performance of our proposed model, we conduct the experimental evaluations on two popular challenging benchmark datasets for aerial image object detection, namely VisDrone [48] and DOTA [49] datasets. The VisDrone consists of 10209 aerial images (6471 for training, 548 for validation and 3190 for testing) with a pixel size of about  $2000 \times 1500$  pixels, the training set of which is manually annotated with 540k instance bounding boxes that are from ten categories of objects. The VisDrone dataset has some problems such as some object being too small, extreme category and scale imbalance and severe target occlusion, which makes it an ideal benchmark for studying small object detection problems. In addition, since the evaluation server is closed now, we can only follow the existing works [10], [8], [9], [20] to use the validation set for evaluation performance. The DOTA dataset is composed of satellite images, including 1411 training images and 458 validation images. It contains roughly 280k manually annotated instances being from the fifteen different categories

of objects, such as planes, ships, large vehicles, helicopters, etc.

**Evaluation metric.** Following the standard evaluation protocol that proposed in MS COCO [50], we report six evaluation metrics, namely  $AP$ ,  $AP_{50}$ ,  $AP_{75}$ ,  $AP_s$ ,  $AP_m$  and  $AP_l$ , to measure the performance of different models. Specifically,  $AP$  is the average precision under multiple IoU thresholds, ranging from 0.5 to 0.95 with a step size of 0.05. The  $AP_s$ ,  $AP_m$  and  $AP_l$  are respectively average precision for small (less than  $32 \times 32$  pixel size), medium and large (larger than  $96 \times 96$  pixel size) objects, which are suitable to study the performance of different methods for small object detection.

##### B. Implementation details

In this paper, all the experiments of our proposed method are run on a single NVIDIA A100 GPU with 40G RAM and implemented based on Detectron2 toolkit<sup>1</sup>. For our experimental validation, we use Faster RCNN as the baseline object detector and its backbone adopts the ResNet50 with FPN that pre-trained on ImageNet dataset. In this paper, our proposed two new modules are plug-and-play type and they can be applied to most existing object detectors, such as CZ Det [10], ClusterNet [8], DensityMap [9], etc. Thus, in order to more fully verify the effectiveness of our proposed new modules in the experiments, we inserted our proposed new modules into three object detection models mentioned above and compared them with the original baseline models. For data augmentation and hyper-parameters, we adopt the same setup with the original baseline models. For VisDrone and DOTA datasets, the model was respectively trained for 180k and 100k iterations. The initial learning rate is both set to 0.007071 and

<sup>1</sup><https://github.com/facebookresearch/detectron2>

respectively decayed by 10 at 100k and 140k iterations and at the 40k-th and 70k-th epoch.

### C. Comparison between our SLPA and the existing CBAM

In order to verify the effectiveness of our proposed SLPA module, Table I gives a comparison between our SLPA module and the existing CBAM (it is a mixture attention model, composing of spatial and channel-wise attention modules) on the VisDrone dataset. Here, we select the CZ Det [10] as our baseline and its object detector (Faster RCNN) adopts the ResNet50 with FPN as the backbone. Baseline+CBAM represents that the CBAM is plugged into each stage of ResNet50 and Baseline+SLPA indicated that our proposed SLPA module is integrated into each stage of ResNet50. Seeing from the Table I, we find that the performance of our proposed SLPA module is superior to that of the CABM, especially for small and middle objects. The possible reason is that our proposed SLPA that employed a pyramid mechanism induced by convolutions with different expansion rates, is better at capturing the fine-grained features of small and medium-sized targets.

### D. Ablation study

In this subsection, we select the CZ Net as the baseline and design a number of ablation studies to analyze the contribution of our proposed modules from different aspects. All the experiments are performed on the VisDrone dataset and the resolution of the input image is  $1200 \times 1999$ .

**Effect of each module.** In Table II, we compare the impact of incorporating our proposed modules into the baseline model on its performance. We observe that the AP score of the baseline raises by 1.1% after only integrating our proposed SLPA module into it. Notably for small and medium-sized objects, the AP scores increase by 1.0% and 1.3%, respectively, surpassing the 0.8% improvement observed in large objects. This result suggests that our proposed SLPA module can improve the features representation ability of the backbone network by the Laplacian Pyramid attention mechanism, especially for small and medium-sized object. When only adding the MSFEM into the baseline model, its performance is improved by 1.3 AP, which shows that it is feasible to utilize our proposed MSFEM to enhance the top-level feature map, because it helps the model mine the critical detail information in the image. In addition, seeing from Table II, we also find that the AP Scores of small, medium and large-sized objects have all demonstrated improvements across different magnitudes. Especially for large object, its AP score improves by 1.1%, outperforming the improvements in the small and medium-sized objects. The main reason is that the top-level feature is inherently responsible for detecting large objects. As shown in the Table II, we observe that integrating deformable convolution modules between the layers of the pyramid structure for feature alignment results in a 1.5-percentage-point improvement in the AP score of baseline model. This result, on the other hand, also demonstrates that during the fusion of features across different levels of FPN, the feature misalignment induced by upsampling operations

can significantly degrade the model performance. Meanwhile, we also notice that the AP scores of small and medium-sized objects respectively increase by 1.1% and 1.7% but the one of large objects drops by 1.8%. The possible reason is that because the number of small, medium and large-sized objects in VisDrone dataset is unbalance, the offsets that learned by the deformation convolution are biased toward adapting to small and medium-sized objects rather than the large ones, which leads to a decline in the detection performance of large objects. After integrating the LSPA and MSFEM into the baseline, the AP score of the baseline increases by 1.5%, exceeding the performance of only adding either of two modules, because these two modules work together to provide the model with high-quality feature information (LSPA can enhance local detailed information and MSFEM can enrich multi-scale features). When integrating the LSPA and DCN modules into the baseline model simultaneously, we observe that the AP score of the baseline model increases by 1.9%, and the ones of small, medium and large-sized objects are all improved, which is superior to the results obtained by adding either of the two modules separately. The main reason is that combining two modules makes full use of the local details representation ability of SLPA and the DCN's feature alignment in the fusing process. After adding three modules into the baseline simultaneously, the AP score reaches 35.3%, and other evaluation metrics also achieve the best results. These results fully validate that the mutual cooperation among the three modules can comprehensively enhance the performance of the model.

**Effect of different dilation rates in our SLPA and MSFEM modules.** In Table III, we give the results of different dilation rate configurations in our SLPA module. Seeing the Table III, we note that the performance of SLPA module performs better when its dilation rate configuration is set to  $\{1, 2, 3\}$ , especially for small object, its AP score reaches the peak. For other alternative dilation rate configurations, the overall performance of the SLPA module exhibits fluctuation, with certain key indicators showing a decline (e.g.,  $AP_s$ ), which illustrates that different dilation rate configurations can influence the ability of the SLPA module to capture the detailed features at different scales, and an appropriate dilation rate configuration can enhance its ability to learn the contextual information in the image better, thereby boosting the overall performance of the proposed model. Thus, in our experiments, the dilation rate configuration of the SLPA module is set to  $\{1, 2, 3\}$ .

In addition, Table IV shows the results of different dilation rate configurations in our MSFEM. Seeing from it, we also observe that when the dilation rate configuration of the MSFEM is  $\{1, 2, 3, 4\}$ , its performance performs best. If selecting other dilation rate configuration, the overall performance of the MSFEM has declined to a certain extent, which verifies that different dilation rate configurations are crucial to the multi-scale feature enhancement of the MSFEM and affect its ability to capture and fuse the different scale features. So, we set the dilation rate configuration of the MSFEM to  $\{1, 2, 3, 4\}$  in our experiments.

TABLE I: Comparison between our proposed SLPA module and the CBAM on the VisDrone dataset. The best results are highlighted by the bold.

methods	Input size	AP(%)	$AP_{50}(\%)$	$AP_{75}(\%)$	$AP_s(\%)$	$AP_m(\%)$	$AP_l(\%)$
Baseline	$1200 \times 1999$	33.2	58.3	33.2	26.1	42.6	43.4
Baseline+CBAM	$1200 \times 1999$	33.9	59.0	34.0	26.6	43.5	<b>44.6</b>
Baseline+SLPA	$1200 \times 1999$	<b>34.3</b>	<b>59.5</b>	<b>34.8</b>	<b>26.9</b>	<b>43.9</b>	44.4

TABLE II: Ablation study of three different modules on the VisDrone dataset, conducted by successively incorporating them into the baseline. The best results are highlighted by the bold.

SLPA	MSFEM	DCN	AP(%)	$AP_{50}(\%)$	$AP_{75}(\%)$	$AP_s(\%)$	$AP_m(\%)$	$AP_l(\%)$
			33.2	58.3	33.2	26.1	42.6	43.4
✓			34.3	59.5	34.8	27.1	43.9	44.2
	✓		34.5	59.7	35.0	26.9	43.5	44.5
		✓	34.7	60.1	35.3	27.2	44.3	41.6
✓	✓		34.7	60.3	34.5	27.0	44.0	44.9
✓		✓	35.1	60.6	35.9	27.8	45.0	44.6
	✓	✓	34.8	59.7	35.0	26.9	44.5	45.0
✓	✓	✓	<b>35.3</b>	<b>61.1</b>	<b>36.1</b>	<b>28.0</b>	<b>45.6</b>	<b>45.5</b>

TABLE III: Ablation study of different dilatation rate configurations within our SLPA module. The best results are highlighted by the bold.

Dilatation rates (r)	AP(%)	$AP_{50}(\%)$	$AP_{75}(\%)$	$AP_s(\%)$	$AP_m(\%)$	$AP_l(\%)$
{1,2,3}	<b>34.3</b>	<b>59.5</b>	<b>34.8</b>	<b>27.1</b>	43.9	44.4
{1,2,4}	34.2	59.1	<b>34.8</b>	26.8	43.7	44.1
{1,2,5}	<b>34.3</b>	59.0	<b>34.8</b>	27.0	<b>44.2</b>	44.2
{1,3,5}	34.0	58.9	34.6	26.7	43.8	43.5
{1,3,6}	33.9	58.6	34.6	26.5	44.1	<b>44.5</b>
{1,3,9}	34.0	58.9	34.7	26.7	43.8	44.1

TABLE IV: Ablation study of different dilatation rate configurations within our MSFEM module. The best results are highlighted by the bold.

Dilatation rates (r)	AP(%)	$AP_{50}(\%)$	$AP_{75}(\%)$	$AP_s(\%)$	$AP_m(\%)$	$AP_l(\%)$
{1,2,3,4}	<b>34.5</b>	<b>59.7</b>	<b>35.0</b>	<b>26.9</b>	43.5	<b>44.5</b>
{1,2,3,5}	34.3	59.6	34.2	26.1	43.2	42.6
{1,2,4,6}	34.4	<b>59.7</b>	34.5	26.5	<b>44.1</b>	42.7
{1,3,5,7}	34.1	59.5	34.1	26.0	43.2	42.3

### E. Results

In this subsection, to comprehensively validate the effectiveness of our proposed SLPA and MSFEM modules, we mainly select the CZ Det as the baseline, and compare its performance after adding our proposed modules with other existing state-of-the-art and the most related methods, including one-stage (QueryNet [22], SDPDet [51], Uniform Crop [7] and LMFF-MFEE [52]) and two-stage (ClusterNet [8], DensityMap [9], CDMNet [20], AMRNet [21], GLSAN [19], CascadeNet [54], CZ Det [10] and so on) small object detection methods, on VisDrone2019 and DOTA-v1.0 datasets.

**VisDrone2019.** Table V gives the comparison results on VisDrone2019 dataset. We observe that, under the same input resolution ( $600 \times 1000$ ), the performance of CZ Det is superior to that of some similar methods (e.g., ClusterNet and Density Map), especially for small target, with the AP score increasing by 3.2% and 0.9% respectively. After adopting the improved ResNet50 backbone, namely integrating the proposed SLPA module into each stage of ResNet50, the performance of three model above is improved to a certain extent, specifically for CZ Det, its AP and  $AP_s$  scores respectively raise by 0.7% and

0.8%. This result illustrates that the proposed SLPA module is helpful for improving the performance of object detector because it enhances the feature representation of the backbone (ResNet50), making the model capture the key details in the image. As shown in Table V, the performance of CZ Det is significantly improved when the input resolution follows the setting of  $1200 \times 1999$  as specified in the original CZ Det paper [10], with AP and  $AP_s$  increasing by 4.7% and 5.3%, respectively, compared to those obtained using a  $600 \times 1000$  input resolution. Moreover, there results surpass the AP and  $AP_s$  of CZ Det variant that adopts the improved backbone (ResNet-50+SLPA) and  $600 \times 1000$  input resolution by 4.0% and 4.5%, respectively. The main reason is that the larger input resolution can provide more richer detailed information for detecting the targets, especially the small ones, which is far more useful than using any feature enhancement method. Meanwhile, we also notice that when the CZ Det with  $1200 \times 1999$  input resolution adopts the improved backbone (ResNet-50+SLPA) to be operated, the AP,  $AP_s$ ,  $AP_m$  and  $AP_l$  scores exceed the corresponding results reported in the baseline by 1.1%, 0.8%, 1.3% and 1.0%, respectively. If continuing to integrate

TABLE V: Comparison results on the VisDrone2019 dataset. The symbol \* denotes that the corresponding object detection methods use the improved backbone network, that is, our proposed SLPA module is plugged into each stage of ResNet-50. The symbol † indicates that the results of the corresponding object detection methods after their input image size is adjusted from  $1000 \times 1999$  to  $600 \times 1000$ . ‘MF’ stands for model fusion. The best result of one column is highlighted by the bold.

Methods	Backbone	Input size	AP(%)	$AP_{50}(\%)$	$AP_{75}(\%)$	$AP_s(\%)$	$AP_m(\%)$	$AP_l(\%)$
One-stage methods								
QueryNet [22]	ResNet-50	-	28.3	48.1	28.8	19.8	35.9	40.3
SDPNet [51]	ResNet-50	-	33.7	56.6	34.3	26.7	42.9	45.7
Uniform crop[7]	ResNet-50	$1024 \times 1024$	31.7	56.3	31.6	25.1	40.4	41.1
LMFF-MFEE [52]	YOLOv8s	$640 \times 640$	27.2	44.5	-	-	-	-
Two-stage methods								
ClusterNet [8]	ResNet-50	$600 \times 1000$	26.7	50.6	24.7	17.6	38.9	51.4
ClusterNet*	ResNet-50+SLPA	$600 \times 1000$	26.9	50.7	24.7	17.8	39.0	51.5
DensityMap [9]	ResNet-50	$600 \times 1000$	28.2	47.6	28.9	19.9	39.6	55.8
DensityMap*	ResNet-50+SLPA	$600 \times 1000$	28.5	47.9	29.1	20.1	39.8	55.9
CDMNet [20]	ResNet-50	$600 \times 1000$	29.2	49.5	29.8	20.8	40.7	41.6
AMRNet [21]	ResNet-50	$800 \times 1500$	31.7	-	-	23.0	43.4	58.1
CRENet [53]	Hourglass-104	$1024 \times 1024$	33.7	54.3	33.5	25.6	45.3	<b>58.7</b>
UCGNet [35]	DarkNet-53	-	32.8	53.1	33.9	-	-	-
GLSAN [19]	ResNet-101	$600 \times 1000$	30.7	55.6	29.9	-	-	-
CascadeNet [54]	ResNet-50	-	28.8	47.1	29.3	-	-	-
CascadeNet+MF [54]	ResNet-50	-	30.1	58.0	27.5	-	-	-
CZ Det†	ResNet-50	$600 \times 1000$	28.5	51.5	28.0	20.8	38.1	50.7
CZ Det*†	ResNet-50+SLPA	$600 \times 1000$	29.2	52.0	28.5	21.6	38.4	51.1
CZ Det [10]	ResNet-50	$1000 \times 1999$	33.2	58.3	33.2	26.1	42.6	43.4
CZ Det*	ResNet-50+SLPA	$1000 \times 1999$	34.3	59.5	34.8	26.9	43.9	44.4
CZ Det+ours	ResNet-50+SLPA	$1000 \times 1999$	<b>35.3</b>	<b>61.1</b>	<b>36.1</b>	<b>28.0</b>	<b>45.6</b>	45.5

TABLE VI: Complexity comparison between the CZ Det and the improved CZ Det model with our proposed modules.

Methods	Backbone	FLOPs/G	Params/M	FPS	AP
CZ Det[10]	ResNet-50	213.12	100.7	12.0	33.2
CZ Det+ours	ResNet-50+SLPA	218.22	107.8	11.4	35.3

our proposed MSFEM module and the existing DCN into the CZ Det, there results can be further improved by 1.0%, 1.1%, 1.7% and 1.1%.

Table VI reports the complexity comparison between the CZ Det and the improved CZ Det model with our proposed modules. Compared to the CZ Det, after it adds our proposed modules, the computational load Flops and the number of parameters have slightly increased, and the detection frame rate FPS only drops from 12.0 to 11.4, which is entirely within the acceptable range. The results show that without sacrificing computational efficiency excessively, the proposed modules significantly improve object detection accuracy.

**DOTA-v1.0.** To further verify the effectiveness of the proposed modules, we also compare several different algorithms on DOTA-v1.0, as shown in Table VII. The variant of CZ Det, namely integrating the proposed modules, its AP score reaches 35.0%, which has an improvement compare to the baseline model (CZ Det), especially for small targets, the  $AP_s$  score increases from 18.2% to 20.2%. The results illustrates that the proposed modules help the baseline improve the detection performance of small targets in aerial images, and better adapt to the variations of target size and shape in remote sensing images. For large objects, the ClusterNet performs better than

our model. The reason is probably that our model gets biased to detect small objects, thanks to the additional crops on training.

**Visualization.** In order to clearly and intuitively compare the object detection results of the original CZ Det and the improved CZ Det that integrates our proposed models in this paper, in Figure 4, we show their detection results on several representative scenarios, including high-density crowded and low-light nighttime situations, where the yellow box represents the detected targets while the red dotted-line box contains the new targets detected by the improved CZ Det besides the original detection results. It can be seen from the visualization results that in various scenarios, the improved CZ Det performs the detection performance better. Especially in the severe occlusion and low-light situations, such as nighttime scenes, the improved CZ Det can detect the more targets and reduce the rate of missing detection effectively. The main reason is that our proposed modules can help the model extract more discriminative features of the targets.

## V. CONCLUSION

This paper first analyzes the challenges faced in small object detection and the shortcomings of feature pyramids in this context. We then introduce the SA attention mechanism after each stage of ResNet-50 to enhance the model’s perceptual and representational capabilities, thereby improving small object detection performance. Additionally, we integrate the MSFEM module at the deepest layer of the feature pyramid to enhance the model’s understanding of semantic information and improve feature transfer across different levels, thereby

TABLE VII: Comparison results of the different object detection algorithms on DOTA-v1.0 dataset. The best result of one column is highlighted by the bold.

Methods	Backbone	Input size	AP(%)	AP <sub>50</sub> (%)	AP <sub>75</sub> (%)	AP <sub>s</sub> (%)	AP <sub>m</sub> (%)	AP <sub>l</sub> (%)	FPS
Uniform crop[7]	ResNet-50	1024 × 1024	33.4	54.0	35.6	16.9	36.8	43.7	<b>0.49</b>
ClusterNet [8]	ResNet-50	1000 × 1000	32.2	47.6	<b>39.2</b>	16.6	32.0	<b>50.0</b>	-
CZ Det[10]	ResNet-50	1200 × 1999	34.6	56.9	36.2	18.2	37.8	43.8	0.30
CZ Det+ours	ResNet-50+SLPA	1200 × 1999	<b>35.0</b>	<b>57.6</b>	36.8	<b>20.2</b>	<b>38.3</b>	43.6	0.24



Fig. 4: Visualization results of the original CZ Det (the first row) and the improved CZ Det (the second row) on several representative scene images.

strengthening feature representation. We also add DCN modules between each layer of the feature pyramid to enhance multi-scale feature fusion and feature alignment. Finally, experimental results demonstrate that the improved algorithm achieves superior performance on datasets such as VisDrone, enhancing the original algorithm’s effectiveness in small object detection.

ACKNOWLEDGMENT

This work is supported by the National Natural Science Foundation of China (No.61602288, 62676160), Fundamental Research Program of Shanxi Province (No.202503021211073). The authors also would like to thank the anonymous reviewers for their valuable suggestions.

REFERENCES

[1] S. Ren, K. He, R. Girshick, and J. Sun, “Faster r-cnn: Towards real-time object detection with region proposal networks,” *IEEE transactions on pattern analysis and machine intelligence*, vol. 39, no. 6, pp. 1137–1149, 2016. 1, 2

[2] J. Redmon, “You only look once: Unified, real-time object detection,” in *Proceedings of the IEEE conference on computer vision and pattern recognition*, 2016. 1, 2

[3] W. Liu, D. Anguelov, D. Erhan, C. Szegedy, S. Reed, C.-Y. Fu, and A. C. Berg, “Ssd: Single shot multibox detector,” in *Computer Vision–ECCV 2016: 14th European Conference, Amsterdam, The Netherlands, October 11–14, 2016, Proceedings, Part I 14*. Springer, 2016, pp. 21–37. 1, 2

[4] H. Law and J. Deng, “Cornernet: Detecting objects as paired keypoints,” in *Proceedings of the European conference on computer vision (ECCV)*, 2018, pp. 734–750. 1, 2

[5] J. Li, X. Liang, Y. Wei, T. Xu, J. Feng, and S. Yan, “Perceptual generative adversarial networks for small object detection,” in *Proceedings of the IEEE conference on computer vision and pattern recognition*, 2017, pp. 1222–1230. 1, 2

[6] Y. Bai, Y. Zhang, M. Ding, and B. Ghanem, “Sod-mtgan: Small object detection via multi-task generative adversarial network,” in *Computer Vision ECCV*, 2018, pp. 210–226. 1, 2

[7] F. Ozge Unel, B. O. Ozkalayci, and C. Cigla, “The power of tiling for small object detection,” in *Proceedings of the IEEE/CVF conference on computer vision and pattern recognition workshops*, 2019, pp. 0–0. 1, 8, 9, 10

[8] F. Yang, H. Fan, P. Chu, E. Blasch, and H. Ling, “Clustered object detection in aerial images,” in *Proceedings of the IEEE/CVF international conference on computer vision*, 2019, pp. 8311–8320. 1, 2, 3, 6, 8, 9, 10

[9] C. Li, T. Yang, S. Zhu, C. Chen, and S. Guan, “Density map guided object detection in aerial images,” in *proceedings of the IEEE/CVF conference on computer vision and pattern recognition workshops*, 2020, pp. 190–191. 1, 2, 3, 6, 8, 9

[10] A. Meethal, E. Granger, and M. Pedersoli, “Cascaded zoom-in detector for high resolution aerial images,” in *Proceedings of the IEEE/CVF Conference on Computer Vision and Pattern Recognition*, 2023, pp. 2046–2055. 1, 2, 3, 6, 7, 8, 9, 10

[11] J. Hu, L. Shen, and G. Sun, “Squeeze-and-excitation networks,” in *Proceedings of the IEEE conference on computer vision and pattern recognition*, 2018, pp. 7132–7141. 2, 3

[12] L. Chen, H. Zhang, J. Xiao, L. Nie, J. Shao, W. Liu, and T.-S. Chua, “Sca-cnn: Spatial and channel-wise attention in convolutional networks for image captioning,” in *Proceedings of the IEEE conference on computer vision and pattern recognition*, 2017, pp. 5659–5667. 2

[13] S. Woo, J. Park, J.-Y. Lee, and I. S. Kweon, “Cbam: Convolutional block attention module,” in *Proceedings of the European conference on computer vision (ECCV)*, 2018, pp. 3–19. 2, 3

[14] S. Anwar and N. Barnes, “Densely residual laplacian super-resolution,” *IEEE Transactions on Pattern Analysis and Machine Intelligence*, vol. 44, no. 3, pp. 1192–1204, 2020. 2, 3, 4

[15] R. Girshick, “Fast r-cnn,” *arXiv preprint arXiv:1504.08083*, 2015. 2

[16] R. Girshick, J. Donahue, T. Darrell, and J. Malik, “Rich feature hierarchies for accurate object detection and semantic segmentation,” in *Proceedings of the IEEE conference on computer vision and pattern recognition*, 2014, pp. 580–587. 2

[17] Z. Tian, C. Shen, H. Chen, and T. He, “Fcos: Fully convolutional one-stage object detection. arxiv 2019,” *arXiv preprint arXiv:1904.01355*, 2019. 2

- [18] T.-Y. Ross and G. Dollár, “Focal loss for dense object detection,” in *proceedings of the IEEE conference on computer vision and pattern recognition*, 2017, pp. 2980–2988. [2](#)
- [19] S. Deng, S. Li, K. Xie, W. Song, X. Liao, A. Hao, and H. Qin, “A global-local self-adaptive network for drone-view object detection,” *IEEE Transactions on Image Processing*, vol. 30, pp. 1556–1569, 2020. [2](#), [8](#), [9](#)
- [20] C. Duan, Z. Wei, C. Zhang, S. Qu, and H. Wang, “Coarse-grained density map guided object detection in aerial images,” in *Proceedings of the IEEE/CVF International Conference on Computer Vision*, 2021, pp. 2789–2798. [2](#), [3](#), [6](#), [8](#), [9](#)
- [21] Z. Wei, C. Duan, X. Song, Y. Tian, and H. Wang, “Amrnet: Chips augmentation in aerial images object detection. arxiv 2020,” *arXiv preprint arXiv:2009.07168*. [2](#), [8](#), [9](#)
- [22] C. Yang, Z. Huang, and N. Wang, “Querydet: Cascaded sparse query for accelerating high-resolution small object detection,” in *Proceedings of the IEEE/CVF Conference on computer vision and pattern recognition*, 2022, pp. 13 668–13 677. [2](#), [8](#), [9](#)
- [23] C. Liu, G. Gao, Z. Huang, Z. Hu, Q. Liu, and Y. Wang, “Yolc: You only look clusters for tiny object detection in aerial images,” *IEEE Transactions on Intelligent Transportation Systems*, vol. 25, no. 10, pp. 13 863–13 875, 2024. [2](#)
- [24] K. Duan, S. Bai, L. Xie, H. Qi, Q. Huang, and Q. Tian, “Centernet: Keypoint triplets for object detection,” in *Proceedings of the IEEE/CVF international conference on computer vision*, 2019, pp. 6569–6578. [2](#)
- [25] Z. Yang, S. Liu, H. Hu, L. Wang, and S. Lin, “Reppoints: Point set representation for object detection,” in *Proceedings of the IEEE/CVF international conference on computer vision*, 2019, pp. 9657–9666. [2](#)
- [26] T.-Y. Lin, P. Dollár, R. Girshick, K. He, B. Hariharan, and S. Belongie, “Feature pyramid networks for object detection,” in *Proceedings of the IEEE conference on computer vision and pattern recognition*, 2017, pp. 2117–2125. [2](#), [3](#)
- [27] Y. Li, Y. Chen, N. Wang, and Z. Zhang, “Scale-aware trident networks for object detection,” in *Proceedings of the IEEE/CVF international conference on computer vision*, 2019, pp. 6054–6063. [2](#), [3](#)
- [28] M. Najibi, B. Singh, and L. S. Davis, “Autofocus: Efficient multi-scale inference,” in *Proceedings of the IEEE/CVF international conference on computer vision*, 2019, pp. 9745–9755. [2](#)
- [29] Z. Liu, G. Gao, L. Sun, and Z. Fang, “Hrdnet: High-resolution detection network for small objects,” in *2021 IEEE international conference on multimedia and expo (ICME)*. IEEE, 2021, pp. 1–6. [2](#)
- [30] R. A. Nihal, B. Yen, K. Itoyama, and K. Nakadai, “From blurry to brilliant detection: Yolov5-based aerial object detection with super resolution,” *arXiv preprint arXiv:2401.14661*, 2024. [2](#)
- [31] Z. Ye, C. Lan, M. Zou, X. Qiu, and J. Chen, “Cca-fpn: Channel and content adaptive object detection,” *Journal of Visual Communication and Image Representation*, vol. 95, p. 103903, 2023. [2](#)
- [32] S. Bell, C. L. Zitnick, K. Bala, and R. Girshick, “Inside-outside net: Detecting objects in context with skip pooling and recurrent neural networks,” in *Proceedings of the IEEE conference on computer vision and pattern recognition*, 2016, pp. 2874–2883. [2](#)
- [33] J.-S. Lim, M. Astrid, H.-J. Yoon, and S.-I. Lee, “Small object detection using context and attention,” in *2021 international Conference on Artificial intelligence in information and Communication (ICAIIIC)*. IEEE, 2021, pp. 181–186. [2](#)
- [34] X. Chen and A. Gupta, “Spatial memory for context reasoning in object detection,” in *Proceedings of the IEEE international conference on computer vision*, 2017, pp. 4086–4096. [2](#)
- [35] J. Liao, Y. Piao, J. Su, G. Cai, X. Huang, L. Chen, Z. Huang, and Y. Wu, “Unsupervised cluster guided object detection in aerial images,” *IEEE Journal of Selected Topics in Applied Earth Observations and Remote Sensing*, vol. 14, pp. 11 204–11 216, 2021. [2](#), [9](#)
- [36] O. C. Koyun, R. K. Keser, I. B. Akkaya, and B. U. Töreyn, “Focus-and-detect: A small object detection framework for aerial images,” *Signal Processing: Image Communication*, vol. 104, p. 116675, 2022. [2](#)
- [37] J. Xu, Y. Li, and S. Wang, “Adazoom: Adaptive zoom network for multi-scale object detection in large scenes,” *arXiv preprint arXiv:2106.10409*, 2021. [2](#)
- [38] H. Li, Y. Liu, W. Ouyang, and X. Wang, “Zoom out-and-in network with map attention decision for region proposal and object detection,” *International Journal of Computer Vision*, vol. 127, pp. 225–238, 2019. [3](#)
- [39] L.-C. Chen, Y. Yang, J. Wang, W. Xu, and A. L. Yuille, “Attention to scale: Scale-aware semantic image segmentation,” in *Proceedings of the IEEE conference on computer vision and pattern recognition*, 2016, pp. 3640–3649. [3](#)
- [40] X. Wang, R. Girshick, A. Gupta, and K. He, “Non-local neural networks,” in *Proceedings of the IEEE conference on computer vision and pattern recognition*, 2018, pp. 7794–7803. [3](#)
- [41] H. Hu, J. Gu, Z. Zhang, J. Dai, and Y. Wei, “Relation networks for object detection,” in *Proceedings of the IEEE conference on computer vision and pattern recognition*, 2018, pp. 3588–3597. [3](#)
- [42] J. Cao, Q. Chen, J. Guo, and R. Shi, “Attention-guided context feature pyramid network for object detection,” *arXiv preprint arXiv:2005.11475*, 2020. [3](#)
- [43] S. Liu, L. Qi, H. Qin, J. Shi, and J. Jia, “Path aggregation network for instance segmentation,” in *Proceedings of the IEEE conference on computer vision and pattern recognition*, 2018, pp. 8759–8768. [3](#)
- [44] M. Tan, R. Pang, and Q. V. Le, “Efficientdet: Scalable and efficient object detection,” in *Proceedings of the IEEE/CVF conference on computer vision and pattern recognition*, 2020, pp. 10 781–10 790. [3](#)
- [45] C. Guo, B. Fan, Q. Zhang, S. Xiang, and C. Pan, “Augfpn: Improving multi-scale feature learning for object detection,” in *Proceedings of the IEEE/CVF conference on computer vision and pattern recognition*, 2020, pp. 12 595–12 604. [3](#)
- [46] X. Zou, F. Xiao, Z. Yu, Y. Li, and Y. J. Lee, “Delving deeper into anti-aliasing in convnets,” *International Journal of Computer Vision*, vol. 131, no. 1, pp. 67–81, 2023. [5](#)
- [47] F. Yu and V. Koltun, “Multi-scale context aggregation by dilated convolutions,” in *ICLR*, 2016. [5](#)
- [48] D. Du, P. Zhu, L. Wen, X. Bian, H. Lin, Q. Hu, T. Peng, J. Zheng, X. Wang, Y. Zhang *et al.*, “Visdrone-det2019: The vision meets drone object detection in image challenge results,” in *Proceedings of the IEEE/CVF international conference on computer vision workshops*, 2019, pp. 0–0. [6](#)
- [49] G.-S. Xia, X. Bai, J. Ding, Z. Zhu, S. Belongie, J. Luo, M. Datcu, M. Pelillo, and L. Zhang, “Dota: A large-scale dataset for object detection in aerial images,” in *Proceedings of the IEEE conference on computer vision and pattern recognition*, 2018, pp. 3974–3983. [6](#)
- [50] T.-Y. Lin, M. Maire, S. Belongie, J. Hays, P. Perona, D. Ramanan, P. Dollár, and C. L. Zitnick, “Microsoft coco: Common objects in context,” in *European conference on computer vision*. Springer, 2014, pp. 740–755. [6](#)
- [51] N. Yin, C. Liu, R. Tian, and X. Qian, “Sdpdet: Learning scale-separated dynamic proposals for end-to-end drone-view detection,” *IEEE Transactions on Multimedia*, vol. 26, pp. 7812–7822, 2024. [8](#), [9](#)
- [52] G. Zhou, Q. Xu, Y. Liu, Q. Liu, A. Ren, X. Zhou, H. Li, and J. Shen, “Lightweight multiscale feature fusion and multireceptive field feature enhancement for small object detection in the aerial images,” *IEEE Transactions on Geoscience and Remote Sensing*, vol. 63, pp. 1–13, 2025. [8](#), [9](#)
- [53] Y. Wang, Y. Yang, and X. Zhao, “Object detection using clustering algorithm adaptive searching regions in aerial images,” in *European Conference on Computer Vision*, 2020, pp. 651–664. [9](#)
- [54] X. Zhang, E. Izquierdo, and K. Chandramouli, “Dense and small object detection in uav vision based on cascade network,” in *Proceedings of the IEEE/CVF International Conference on Computer Vision Workshops*, 2019, pp. 0–0. [8](#), [9](#)



**Zhangjian Ji** received the B.S. degree from Wuhan University, China, in 2007, the M.E. degrees from the Institute of Geodesy and Geophysics, Chinese Academy of Sciences (CAS), China, in 2010, and the Ph.D. degree in the University of Chinese Academy of Sciences, China, in 2015.

He is currently an Associate Professor at the School of Computer and Information Technology, Shanxi University, Taiyuan, China. His research interests include computer vision, pattern recognition, machine learning and human-computer interaction.



**Huijia Yan** received the M.E. degrees in Computer technologies from Shanxi university, China, in 2025.

His research interests include computer vision, object detection, etc.



**Shaotong Qiao** received the B.S. degree in engineering from Shandong Jianzhu University, China, in 2024. He is currently pursuing the M.E. degrees in Computer technologies from Shanxi university, China.

His research interests include computer vision, person re-identification, etc.



**Kai Feng** received the Ph.D. degree in science from Shanxi University, China, in 2014. He is currently an Associate Professor at the School of Computer and Information Technology, Shanxi University, Taiyuan, China.

His research interests include combinatorial optimization and interconnection network analysis.



**Wei Wei** (Member, IEEE) received the PhD degree in computer science from Shanxi University, in 2012. He is currently a full professor with the School of Computer and Information Technology, Shanxi University.

He has authored or coauthored more than 40 papers in his research fields, including the IEEE TPAMI, IEEE TKDE, NeurIPS, ICML, AAAI, IJ-CAI, and so on. His current research interests include data mining, machine learning, and embodied intelligence.